

## Clusters of Amphiphilic Colloidal Spheres

Liang Hong,<sup>†</sup> Angelo Cacciuto,<sup>†</sup> Erik Luijten,\* and Steve Granick\*

Department of Materials Science and Engineering, University of Illinois, Urbana, Illinois 61801

Received October 4, 2007. In Final Form: November 28, 2007

Orientation-dependent interactions can drive unusual self-assembly of colloidal particles. This study, based on combined epifluorescence microscopy and Monte Carlo simulations, shows that amphiphilic colloidal spheres, hydrophobic on one hemisphere and charged on the other, assemble in water into extended structures not formed by spheres of uniform surface chemical makeup. Small, compact clusters each comprised of less than 10 of these Janus spheres link up, as increasing salt concentration enhances electrostatic screening, into wormlike strings.

### Introduction

The Nobel Prize address of P.-G. de Gennes called attention to the exciting potential, in science and technology, of “Janus” spheres whose chemical makeup differs between the two hemispheres.<sup>1</sup> The idea was largely ignored at the time, however. Indeed, though magnetic effects comprise an obvious counterexample to the assumption of isotropic particle–particle interactions, studies of magnetic colloids have proceeded essentially independently. The ensuing years saw colloid science mature impressively in the different direction of using colloids to emulate atomic systems where the homogeneous chemical makeup of the elements in the system is essential.<sup>2–6</sup> Not until nearly a generation later was the Janus particle concept extended by several theory groups and by perspective articles to propose the vision of “molecular colloids” whose patchy surface chemical makeup governs their assembly into superstructures.<sup>7–11</sup> The assembly of larger (non-Brownian) objects was also considered.<sup>12,13</sup> This proposal was revolutionary because the assumption that the relevant interactions between colloids are nondirectional is presently the premise for analyzing a vast number of ubiquitous technological, environmental, and energy-related problems involving colloids.<sup>14,15</sup> In contrast, the interaction potential between Janus particles depends not only on separation but also on their relative orientation.<sup>16</sup> The combined experimental and simulation study presented below implements this vision in the simple, generalizable system of amphiphilic solid spheres:

colloids whose two hemispheres are hydrophobic and charged, respectively, thereby comprising *solid* surfactants that assemble into clusters and other structures not formed by spheres of uniform surface chemical makeup.

Ironically, the concept of directional (nonmagnetic) interactions between spheres has a venerable history from the standpoint of theory and simulation. The notion of sticky spots was mentioned by Boltzmann in the analysis of gases,<sup>17</sup> and it is over a century old. During the last 20 years, it saw much development in other contexts, especially directional interactions in hard-sphere fluids<sup>18</sup> and between proteins,<sup>19</sup> even before the more recent developments in the colloid field.<sup>7–11</sup> The main new point of the present study is to show striking agreement between simulation and experiment regarding the simple, generic, and generalizable systems discussed below, especially the development of wormlike strings from building blocks comprised of smaller compact clusters.

The property of being amphiphilic drives molecules to self-assemble into a large family of superstructures that are integral to many of the most useful and complex features of soft materials. Among synthetic amphiphilic molecules, prominent examples include not only surfactants and detergents<sup>14,15</sup> but also the burgeoning use of block copolymers in technology.<sup>20,21</sup> In biology, self-assembly of phospholipids into biological membranes follows similar elemental principles, although those systems present the added complexity of containing mixtures of many different sorts of amphiphilic molecules.<sup>22</sup>

A simple thought experiment gives intuitive insight into the origin of the range of self-assembled structures revealed by the more detailed experiments and simulations that we describe below. Consider pairs of amphiphilic colloid-sized spheres in water at a fixed separation but various orientations (Figure 1A). It is obvious that the interaction potential switches from an extreme of attraction when the hydrophobic sides face one another to an extreme of repulsion when the charged sides face one another, and takes intermediate values in between. There is also a more subtle dependence on ionic strength (Figure 1B). Ignoring for the moment the hydrophobic attraction, which is believed to be

\* To whom correspondence should be addressed. E-mail: luijten@uiuc.edu (E.L.); sgranick@uiuc.edu (S.G.).

<sup>†</sup> These authors contributed equally.

- (1) de Gennes, P.-G. *Rev. Mod. Phys.* **1992**, *64*, 645.
- (2) Weeks, E. R.; Crocker, J. C.; Levitt, A. C.; Schofield, A.; Weitz, D. A. *Science* **2000**, *287*, 627.
- (3) Manoharan, V. N.; Elsesser, M. T.; Pine, D. J. *Science* **2003**, *301*, 483.
- (4) Alsayed, A. M.; Islam, M. F.; Zhang, J.; Collings, P. J.; Yodh, A. G. *Science* **2005**, *309*, 1207.
- (5) Leunissen, M. E.; Christova, C. G.; Hynninen, A. P.; Royall, C. P.; Campbell, A. I.; Imhof, A.; Dijkstra, M.; van Roij, R.; van Blaaderen, A. *Nature* **2005**, *437*, 235.
- (6) Savage, J. R.; Blair, D. W.; Levine, A. J.; Guyer, R. A.; Dinsmore, A. D. *Science* **2006**, *314*, 795.
- (7) Zhang, Z. L.; Glotzer, S. C. *Nano Lett.* **2004**, *4*, 1407.
- (8) de Michele, C.; Gabrielli, S.; Tartaglia, P.; Sciortino, F. *J. Phys. Chem. B* **2006**, *110*, 8064.
- (9) Van Workum, K.; Douglas, J. F. *Phys. Rev. E* **2006**, *73*, 031502.
- (10) van Blaaderen, A. *Nature* **2006**, *439*, 927.
- (11) Edwards, E. W.; Wang, D. Y.; Möhwal, H. *Macromol. Chem. Phys.* **2007**, *208*, 439.
- (12) Terfort, A.; Bowden, N.; Whitesides, G. M. *Nature* **1997**, *386*, 162.
- (13) Onoe, H.; Matsumoto, K.; Shimoyama, I. *Small* **2007**, *3*, 1383.
- (14) Israelachvili, J. N. *Intermolecular and Surface Forces*, 2nd ed.; Academic Press: New York, 1991.
- (15) Lyklema, J. *Fundamentals of Colloid and Interface Science*; Academic: San Diego, CA, 2005; Vol. 4.
- (16) Hong, L.; Cacciuto, A.; Luijten, E.; Granick, S. *Nano Lett.* **2006**, *6*, 2510.

(17) Boltzmann, L. *Vorlesungen über Gas theorie II*; J. A. Barth: Leipzig, 1898 [Lectures on Gas Theory; Brush, S. G., transl.; University of California Press: Berkeley, CA, 1964; Part II, Chapter 6].

(18) Wertheim, M. S. *J. Chem. Phys.* **1986**, *85*, 2929.

(19) Lomakin, A.; Asherie, N.; Benedek, G. B. *Proc. Natl. Acad. Sci. U.S.A.* **1999**, *96*, 9465.

(20) Jain, S.; Bates, F. S. *Science* **2003**, *300*, 460.

(21) Discher, B. M.; Won, Y. Y.; Ege, D. S.; Lee, J. C. M.; Bates, F. S.; Discher, D. E.; Hammer, D. A. *Science* **1999**, *284*, 1143.

(22) Lodish, H.; Berk, A.; Zipursky, S. L.; Matsudaira, P.; Baltimore, D.; Darnell, J. *Molecular Cell Biology*, 4th ed.; W. H. Freeman & Co: New York, 2000.

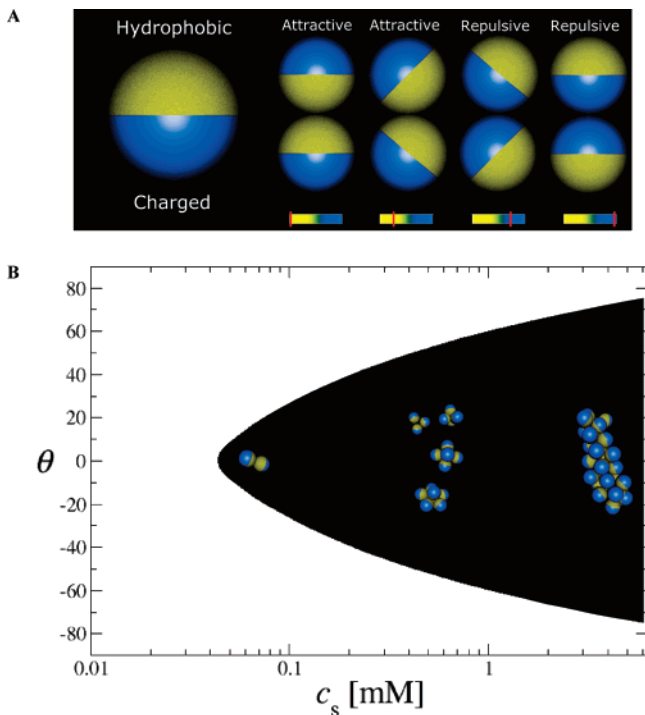


**Figure 1.** (A) Pairs of colloidal particles in water, each hydrophobic on one hemisphere and charged on the other (denoted by yellow and blue colors), are considered at fixed separation. The interaction potential switches from attractive when the hydrophobic sides face one another (left) to repulsive when the charged sides face one another (right), with intermediate attraction or repulsion at canted angles (middle). Below each particle pair, the intensity of the interaction potential at that mutual orientation is shown schematically. (B) Region of permitted tilt angles between two charged hemispheres with  $1 \mu\text{m}$  diameter held at a center-to-center distance of  $1.020$  micrometers, plotted as a function of the logarithmic concentration of monovalent salt. The boundary is determined by requiring the electrostatic energy cost per simultaneous rotation of the particles over an angle  $\theta$  to be smaller than  $1 k_B T$ . The reference angle  $\theta = 0$  refers to the leftmost pair in the top panel, where the hydrophobic hemispheres face one another. The structures within the bottom panel illustrate the range of structures considered in more detail in Figures 3 and 4.

insensitive to or only weakly dependent on ionic strength,<sup>23</sup> consider the allowed angles between two amphiphilic particles in near-proximity under conditions described in the figure caption. In the limit of very low ionic strength, electrostatic repulsion is so severe that the particles must strongly repel one another regardless of orientation, but this weakens significantly when the electrostatic screening length becomes less than the particle size. Initially, the colloids will orient such that the charged hemispheres are diametrically opposite, but this restriction is loosened with increasing ionic strength. In Figure 1B, we quantify the permitted tilt angles according to the criterion that the electrostatic energy cost of a simultaneous rotation (within the same plane) of both particles over an angle  $\theta$  with respect to their center-to-center axis is less than  $1 k_B T$  ( $k_B$  is Boltzmann's constant and  $T$  is the absolute temperature); one sees that the higher the ionic strength, the greater the range of allowed angles. This allows more complex shapes when the particles assemble spontaneously into clusters, as will be shown below.

### Experimental and Computational Details

On the experimental side, to prepare amphiphilic colloidal spheres, fluorescent carboxylate-modified polystyrene spheres

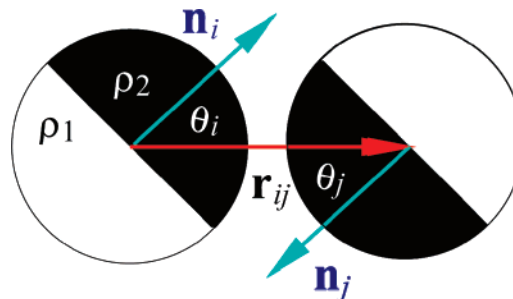


**Figure 2.** Configuration of two Janus particles in close proximity. The black hemisphere represents the hydrophobic side, whereas the white hemisphere is charged. This graph illustrates the center-to-center axis  $r_{ij}$  and the polar axes  $n_i$  and  $n_j$  used in the Monte Carlo simulations.

are spread onto a cleaned glass slide and coated on the exposed hemisphere with a thin (30 nm) film of gold. Subsequently, a monolayer of octadecanethiol (ODT) is assembled on the gold using conventional thiol chemistry. The untreated hemisphere has a high negative charge density resulting from carboxylic acid groups on the parent colloidal sphere. To further increase this negative charge density, in some experiments, DNA oligomers are grafted on the surface using a conjugation reaction described in the literature,<sup>24</sup> such that after DNA grafting each of the 22 bases carries one negative charge. The particles (F8819 from Invitrogen, Inc.) have a  $1 \mu\text{m}$  diameter, although we believe that size is not fundamental as long as it exceeds the electrostatic screening length. The particles are then suspended in aqueous solution and settle to the bottom of the glass sample container. Using epifluorescence microscopy, we image a thin region  $\approx 5 \mu\text{m}$  from the surface, where the particle concentration is relatively high, although the maximum volume fraction is still only around  $10^{-3}$ . When the ionic strength is varied, this is done by adding  $\text{KNO}_3$ .

To prepare the hydrophobic patch on the spheres, a suspension of (fluorescent) carboxylate-modified polystyrene spheres is spread onto a cleaned glass slide such that a monolayer of colloids remains after the suspension liquid evaporates. A thin (30 nm) film of gold is deposited using electron beam deposition onto a titanium adhesion-promoting layer (2 nm). Onto the gold hemisphere surfaces, monolayers of octadecanethiol (ODT) are deposited and washed multiple times first with 1% HCl-ethanol solution and then with deionized water to remove nonspecific adsorption. The other, untreated, hemisphere remains coated with negative charges from the carboxylic acid groups on the parent spheres. The resulting amphiphilic spheres are then removed from the surface using ultrasonication. In experiments where the negative charge resides simply on native carboxylate groups, the particles are used directly. In experiments where DNA oligomers are grafted to the polar hemisphere to raise the negative charge, the carboxylic acid groups on the particle surfaces are activated using 1-ethyl-3-(3-dimethylaminopropyl) carbodiimide hydrochloride (EDC) in 2-morpholinoethanesulfonic acid at pH = 4.5 using 2-(*N*-morpholino)ethanesulfonic acid (MES) buffer solution, and then these activated groups are allowed to react with the amino termini of DNA. It is convenient to use the DNA heptamer 5'-TAC GAG TTG AGA TTT TTT TTT T/iSP18/3AmM/-3'. After reaction, unreacted DNA is removed by washing first in 2% Tween 20 solution and then pH 7.5 phosphate-buffered saline (PBS) buffer. The resulting particles are placed in deionized water. A control experiment showed that the other hemisphere remained hydrophobic.

(23) Meyer, E. E.; Rosenberg, K. J.; Israelachvili, J. *Proc. Natl. Acad. Sci. U.S.A.* **2006**, *103*, 15739.

(24) Rogers, P. H.; Michel, E.; Bauer, C. A.; Vanderet, S.; Hansen, D.; Roberts, B. K.; Calvez, A.; Crews, J. B.; Lau, K. O.; Wood, A.; Pine, D. J.; Schwartz, P. V. *Langmuir* **2005**, *21*, 5562.

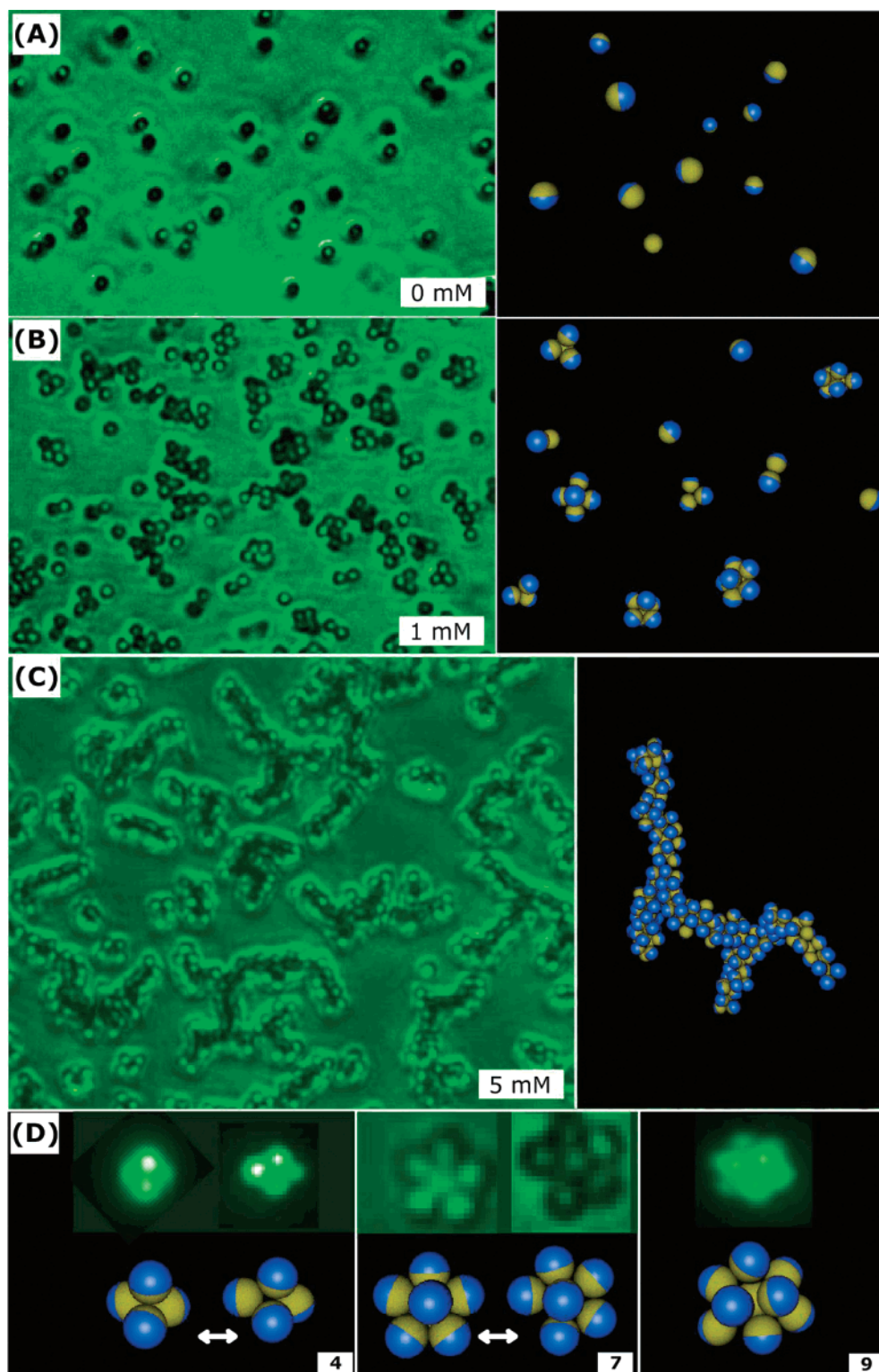


**Figure 3.** Varying the salt concentration causes amphiphilic particles ( $1 \mu\text{m}$  diameter) to assemble into clusters of various sizes and shapes. The images with green background represent epifluorescence experiments. In the Monte Carlo computer simulations, blue and yellow colors represent charged and hydrophobic hemispheres, respectively. Panel (A) shows discrete particles for the case of particles in deionized water. Panel (B) ( $1 \text{ mM KNO}_3$ ) shows small clusters (up to nonahedra) in equilibrium with one another. Panel (C) ( $5 \text{ mM KNO}_3$ ) shows long, branched wormlike strings. The simulations (right) confirm that the assembly of small clusters into strings occurs as the range of the electrostatic repulsion, relative to hydrophobic attraction, decreases with increasing salt. Panel (D) shows further comparison of epifluorescence images and Monte Carlo simulations with excellent agreement. Experimentally, clusters with the same number of particles ( $N$ ) interconvert dynamically between different shapes, as confirmed from simulations for tetramers,  $N = 4$  (left), and heptamers,  $N = 7$  (middle). The nonahedral structure,  $N = 9$ , is also confirmed (right).

In the Monte Carlo (MC) computer simulations, we model the amphiphilic nature of the colloidal particles using an interaction potential consisting of three terms: an isotropic repulsive hard-core potential to prevent particle overlap, a hydrophobic attraction

$V_H$  between the nonpolar hemispheres, and an electrostatic repulsion  $V_E$  between the polar sides of the particles. In treating the hydrophobic interaction, we adopt a minimalistic model and avoid the controversial question of the mechanism of hydrophobic

attraction,<sup>21</sup> which is not the problem at hand. Instead, we take from the available experiments the conclusion that the attractive hydrophobic interaction is short-ranged compared to our particle diameter, decaying roughly exponentially with interparticle separation  $r_{ij}$  with a decay constant on the order of 10 nm under normal circumstances.<sup>23</sup> We simplify this to an attractive square-well potential with a range of 5% of the particle diameter  $\sigma$  and modulate it to take into account the Janus-like character of the particles. On physical grounds, the magnitude of the interaction is proportional to the effective hydrophobic surface area shared by two particles when facing each other,

$$V_H(r_{ij}, \mathbf{n}_i, \mathbf{n}_j) = \begin{cases} -6I_1(\mathbf{n}_i, \mathbf{n}_j) & \text{if } r_{ij} < 1.05\sigma \\ 0 & \text{otherwise} \end{cases} \quad (1)$$

where  $r_{ij} \equiv |\mathbf{r}_i - \mathbf{r}_j|$  indicates the center-to-center distance between particles  $i$  and  $j$  (which are located at  $\mathbf{r}_i$  and  $\mathbf{r}_j$ , respectively).  $\mathbf{n}_i$  and  $\mathbf{n}_j$  are unit vectors denoting the orientations of the respective particles; as indicated in Figure 2,  $\mathbf{n}$  is parallel to the “polar axis,” where the “northern hemisphere” is hydrophobic. The function  $I_1$  accounts for the fact that only one hemisphere on each particle experiences a hydrophobic attraction,

$$I_1(\mathbf{n}_i, \mathbf{n}_j) = \begin{cases} [(\mathbf{n}_i \cdot \mathbf{r}_{ij})(\mathbf{n}_j \cdot \mathbf{r}_{ji})]^{1/2} & \text{if } \{(\mathbf{n}_i \cdot \mathbf{r}_{ij}) > 0 \wedge (\mathbf{n}_j \cdot \mathbf{r}_{ji}) > 0\} \\ 0 & \text{otherwise} \end{cases} \quad (2)$$

The precise choices for the well depth and range of the attractive interaction are immaterial: the same cluster configurations are found for attractions up to  $10 k_B T$  and interaction ranges up to approximately 10% of the particle diameter.

The screened electrostatic interactions between the charged hemispheres are described by a pairwise Debye–Hückel potential with a distance-dependent interaction again modulated according to the orientation of the particles. It is important to notice that (a) the hydrophilic and the hydrophobic sides of each particle have a very different surface charge density and (b) the range of the electrostatic interaction is short compared to the particle diameter, with typical Debye screening lengths  $\lambda_D$  around 10 nm (as compared to  $\sigma \approx 1 \mu\text{m}$ ). Accordingly, the repulsion between a pair of particles at contact is due almost completely to the charge contained in a spherical cap of area  $2\pi(\sigma/2)\lambda_D = \pi\sigma\lambda_D$ , multiplied by a geometric factor,  $A_0$ , which quantifies to what extent all surface charges contribute to the electrostatic interaction. We obtain this factor by computing the full electrostatic repulsion between two hemispheres decorated with over 20 000 discrete charges each, a number comparable to the estimated number of elementary charges on the colloids used in the experiments. The resulting value for  $A_0$  is typically on the order of  $10^{-2}$ . The angular dependence of the electrostatic potential is quantified by noting that, at fixed interparticle separation, this potential only exhibits a variation with changing relative orientation of the particles when, for either or both of the two particles, the boundary between the two hemispheres is sufficiently close to the region of interaction. Indeed, owing to the rapid change in surface charge density at this boundary and owing to the short range of the screened interaction, for this situation, the pair potential changes quite rapidly as a function of relative orientation. Therefore, we approximate the angular dependence at the Janus interface by a step function. For screening lengths larger than 50 nm, this is no longer a good approximation. However, for these circumstances, the electrostatic repulsion between the particles is so strong that no aggregation is observed at all, and hence, the short-distance details of the potential are irrelevant for our

purposes. Thus, the resulting potential is given by

$$V_E(r_{ij}) = \frac{1}{r_{ij}} A_0 I_2(\mathbf{n}_i, \mathbf{n}_j) \exp[-(r_{ij} - \sigma)/\lambda_D] \quad (3)$$

where the angular dependence is quantified by the function  $I_2$ ,

$$I_2(\mathbf{n}_i, \mathbf{n}_j) = \begin{cases} (\pi\sigma\lambda_D)^2 \rho_1^2 \lambda_B & \text{if } \{(\mathbf{n}_i \cdot \mathbf{r}_{ij}) < 0 \wedge (\mathbf{n}_j \cdot \mathbf{r}_{ji}) < 0\} \\ (\pi\sigma\lambda_D)^2 \rho_1 \rho_2 \lambda_B & \text{if } \{(\mathbf{n}_i \cdot \mathbf{r}_{ij})(\mathbf{n}_j \cdot \mathbf{r}_{ji}) < 0\} \\ (\pi\sigma\lambda_D)^2 \rho_2^2 \lambda_B & \text{if } \{(\mathbf{n}_i \cdot \mathbf{r}_{ij}) > 0 \wedge (\mathbf{n}_j \cdot \mathbf{r}_{ji}) > 0 \wedge r_{ij} > 1.05\sigma\} \\ 0 & \text{if } \{(\mathbf{n}_i \cdot \mathbf{r}_{ij}) > 0 \wedge (\mathbf{n}_j \cdot \mathbf{r}_{ji}) > 0 \wedge r_{ij} < 1.05\sigma\} \end{cases} \quad (4)$$

$\rho_1$  and  $\rho_2$  are the charge densities on the charged and hydrophobic hemispheres, respectively, of each particle.  $\lambda_B = 0.7$  nm is the Bjerrum length. Although it may be argued that the surface charge in the experimental system is more accurately described by constant-potential than by constant-charge boundary conditions, for simplicity we have adopted the latter in our simulations.

Use of this effective functional form allows us to study systems containing several thousands of particles for a large number of steps, which is essential to ensure that stable configurations are reached. The MC simulations employ a standard Monte Carlo algorithm and are all performed in the NVT ensemble with periodic boundary conditions. The minimum-energy states were reached fairly quickly, but to ensure equilibration we continued all runs for a minimum of  $1 \times 10^6$  MC sweeps.

## Results and Discussion

Comparing structures observed in the experiments and computer simulations, the matched images in Figure 3 show pleasing agreement; this indicates that the mechanism of cluster formation is the minimization of free energy. First, in deionized water, the amphiphilic spheres repel one another so strongly that no clusters form (Figure 3A). However, when the electrostatic screening length falls to 10 nm at higher salt concentration (Figure 3B), clusters form with the property that, for each number ( $N$ ) of spheres in the cluster, that cluster possesses a definite, compact structure. When the electrostatic screening length is further reduced a factor 2.2 by adding more salt, the smaller clusters polymerize into extended, branched, wormlike objects (Figure 3C).

Finally, the matched images in Figure 3D illustrate the process of self-assembly for clusters of sizes  $N = 4$ ,  $N = 7$ , and  $N = 9$ . The fluorescence microscopy experiments are unambiguous in revealing equilibration events on time scales of seconds to minutes as these clusters self-assemble: dynamical particle attachment to and detachment from clusters, and reconfiguration of cluster shapes. Indeed, the striking agreement between the experiments and simulations implies that the structures observed experimentally are equilibrated; this is consistent with the fact that from simulation we estimate the particle–particle attraction in experiments to be on the order of only 5–10  $k_B T$ . Some structures, for example, the nonamer ( $N = 9$ ), possess a single stable structure. However, the relatively weak attractive potential and experimental observations of dynamic interconversion between different shapes are consistent with the fact that in the Monte Carlo simulations we observe two distinct configurations for the tetramer ( $N = 4$ ), both of which are observed in the experiments as well. For the heptamer ( $N = 7$ ), we find that while the compact variant (left in Figure 3D) is the most stable, the more “open” arrangement on the right is also observed both experimentally and computationally. The main point is that these clusters possess no definite, frozen shape: they wriggle and rearrange with time.

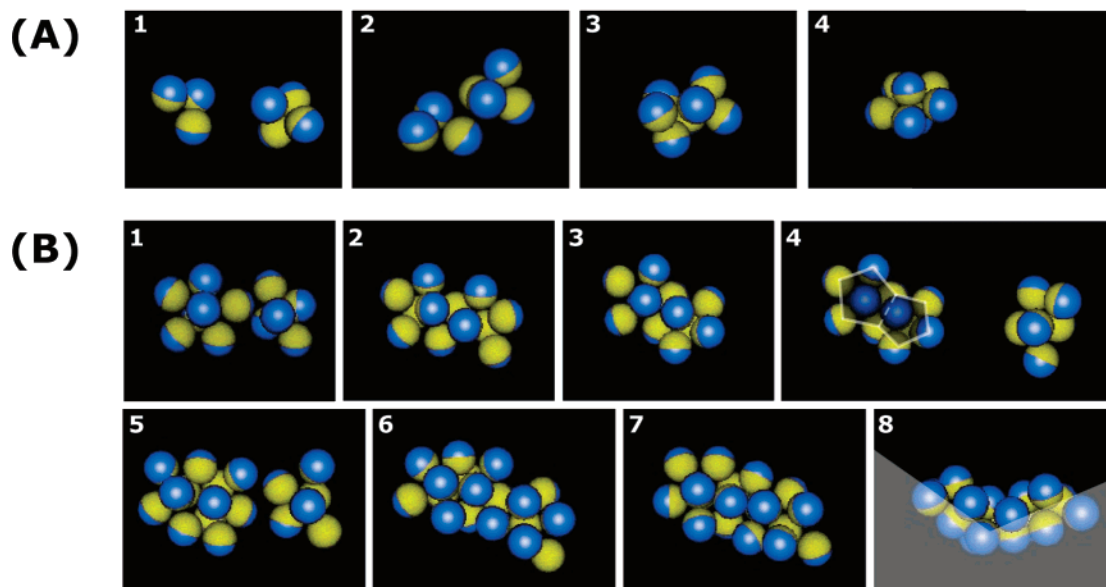


**Figure 4.** Monte Carlo simulations of the polymerization of clusters of amphiphilic spheres into wormlike strings. Assembly proceeds in sequence from left to right. Panel (A) illustrates that, as a trimer ( $N = 3$ ) and tetramer ( $N = 4$ ) approach, particles within these clusters reorient until they fuse together in a lock-and-key structure to form a heptamer ( $N = 7$ ). Panel (B) shows similar fusion of a heptamer and a pentamer (images 1–4), followed by fusion with a hexamer (images 4–7), leading to a kink in the wormlike string (image 8). As the small clusters fuse, individual colloids rearrange to maintain five-fold rings and reorient such that their hydrophobic sides are directed toward the interior of the worm. Specifically, when the  $N = 5$  cluster merges with an  $N = 7$  cluster, two pentagons are formed that are not coplanar (panel B, image 4). When the resulting aggregate incorporates another  $N = 6$  cluster, the individual particles rearrange once more to form a third pentagonal structure (panel B, images 6 and 7). Note that large structures grow through cluster aggregation and not via the stepwise addition of discrete particles.

The significance is to explain the lock-and-key polymerization mechanism that allows wormlike strings to assemble when clusters meet. On this point, experiment and simulation agree that they form not by sequential addition of individual particles, as would be characteristic of molecular surfactants,<sup>14,15</sup> but rather by smaller clusters locking onto one another. We note that, although the Monte Carlo simulations do not reproduce the actual dynamics of the Janus particles, the exclusive use of local particle moves makes it possible to attach a dynamic interpretation to the simulation results. The caption of Figure 4 illustrates the cluster aggregation process in detail. In particular, heptamers, as one of the most stable clusters whose detailed shape nonetheless breathes dynamically (Figure 3D), are a crucial building block for the chain, and Figure 4A shows their formation from the fusion of a trimer and a tetramer. Next, Figure 4B shows how during the fusion of a heptamer with another cluster, such as a pentamer ( $N = 5$ ), the former imprints its topology (a pentagon-shaped arrangement of five colloids flanked by two additional particles) on the latter (cf. panels 1–4 of Figure 4B), leading to the wormlike strings observed in Figure 3C. Also, the characteristic kinks displayed by the strings in the micrographs and MC simulations can be understood from this cluster-aggregation mechanism. One example of such kink formation is illustrated in Figure 4B (panels 5–7): When a hexamer ( $N = 6$ ) meets a string end formed from a heptamer and a pentamer, the latter is distorted as the particles in the hexamer attempt to arrange in a five-fold ring. The frustration arising from simultaneously satisfying the hydrophobic attractions and the electrostatic repulsions causes the string to bend (panel 8). The detailed analysis just presented thus gives insight into the formation mechanisms of the shapes observed in the laboratory (Figure 3C).

The structures described above are analogous to the micellar shapes adopted by standard molecular amphiphiles, although an agenda for future study will be to understand the delicate question of how their shapes evolve from the dilute concentrations considered here to concentrated suspensions. Our findings can be generalized in several ways. Using scale-up methods recently

introduced,<sup>25</sup> a wide range of other particle sizes, as small as 200 nm, can be functionalized to be chemically asymmetric, giving this concept potential application in industrial practice to replace molecular surfactants in certain functions. Furthermore, other self-assembled structures can be expected when the balance is varied between the respective areas of the hydrophobic and hydrophilic patches, and also when solid surfactants of different sizes are mixed. On the applications side, it is expected that solid surfactants of the kind described here will segregate strongly to liquid interfaces, thus stabilizing emulsions and foams. We conjecture that the wormlike strings may also modify suspension rheology as well as possibly serve as vehicles within which to encapsulate cargo for subsequent release.

Looking to the future, extension to particles of a more complex shape than spheres comprises an obvious extension that can be easily implemented. In the same spirit, while this study was restricted to amphiphilicity because it is one of the most pervasive forms of chemical asymmetry, the exploration of more subtle interactions, such as hydrogen bonding, molecular recognition, and the attachment of macromolecules, offers other potential extensions. The idea of having solid surfactants generalizes the concept of molecular amphiphilicity that is so pervasive and useful in nature and technology.

**Acknowledgment.** This paper is dedicated to the late P.-G. de Gennes. We thank M. Shyr and P. V. Braun for assistance in DNA grafting. This work was supported by the U.S. Department of Energy, Division of Materials Science, under Award No. DE-FG02-07ER46471 through the Frederick Seitz Materials Research Laboratory at the University of Illinois at Urbana–Champaign.

LA7030818